FEM analysis of timber-steel hybrid bridge structure

○KISS Lajos*, SASAKI Takanobu**, IIJIMA Yasuo*** and USUKI Seizo****

* Dr. Eng., JSPS Postdoctoral Fellow, Institute of Wood Technology, Akita Pref. University
(11-1 Kaieizaka, Noshiro, Akita 016-0876, Japan)
** Dr. Eng., Associate Professor, Institute of Wood Technology, Akita Pref. University
(11-1 Kaieizaka, Noshiro, Akita 016-0876, Japan)
*** Dr. Agr., Professor, Institute of Wood Technology, Akita Pref. University
(11-1 Kaieizaka, Noshiro, Akita 016-0876, Japan)
****Dr. Eng., Professor, Dept. of Civil and Environmental Engineering, Akita University
(1-1 Tegata, Gakuen-machi, Akita 010-8502, Japan)

ABSTRACT Japanese cedar usage is a major issue in Japan, which is why several research programs concerning civil engineering utilization of this material, for example for guardrails, timber bridges, are under way. The authors aim to develop a highly durable timber bridge by using a Japanese cedar-steel hybrid structure. The authors continue to further investigate the behavior of a proposed glulam beam-steel deck hybrid bridge structure for short and medium span bridges, introduced in their previous works. In this paper, calculated results are presented from an analytical approach using plastic composite beam theory and from a finite element analysis. These are compared to measured results from bending and failure tests.

Keywords: *FEM, glulam beam, orthotropic steel deck, hybrid structure, failure test*

1. INTRODUCTION

Japanese cedar usage is a major issue in Japan, which is why several research programs concerning civil engineering utilization of this material, e.g. guardrails, timber bridges, are under way. The authors aim to develop a highly durable timber bridge by using a Japanese cedar glulam beam-steel deck hybrid structure. One purpose of this comprehensive, ongoing study is to check the agreement between measured results and calculated results from two analytical methods. In this study, the authors continue to further investigate the behavior of the glulam beam-steel deck hybrid bridge structure by continuing their three-dimensional finite analysis[1]. This hybrid structure for short and medium span bridges was introduced by the authors in their previous works[2),3),4)]. A comprehensible design method was necessary to make this bridge structure more available and familiar for clients and bridge designers. Earlier, the authors proposed the use of plastic composite beam theory as a simple, but reliable way of design for this type of bridge. In order to validate the adaptability of this approach for this type of hybrid structure, experimental verification was necessary.

This reason determined the authors to prepare a reduced scale model of the hybrid bridge, initially using Douglas fir glulam material for the main beams and steel for the floor beams. In order to stimulate the use of the widely planted Japanese cedar for structural applications, in a newly designed structure Japanese cedar replaced the Douglas fir: here, Japanese cedar was used not only for the main beams, but also for the floor beams, too. In addition to the simplified analytical approach and testing of the structure, a three-dimensional finite element analysis was necessary. Results from the analytical approach using plastic composite beam theory are presented together with results from the finite element analysis. These are being compared to measured results from bending and failure tests. This paper presents results focusing mainly on the deformed shape, as well as deflection and strain distributions of the hybrid structure, using the three available sets of results, coming from the tests performed, from the plastic composite beam theory and from the FEM analysis.

2. TESTING OF BRIDGE MODEL

The orthotropic steel deck-glulam beam hybrid bridge model was constructed, instrumented and tested to bending and failure at the structural testing laboratory of the Institute of Wood Technology, Akita Prefectural University, situated in Noshiro City, Japan. The tested model was composed of an orthotropic steel deck, attached to two double glulam main beams made of Japanese cedar. It was a reduced model, shown in Fig.1, the scale being one-third of a prototype bridge[4].

Total length is 5.2 m (span is 5.0 m), width is 2067 mm and thickness is t_d = 4.5 mm. The orthotropic steel deck consists of a deck plate, stiffened by eight U-shaped longitudinal ribs and seven double glulam floor beams (60x250 mm each), arranged with an interval of 833 mm. A width variation of each main beam takes place from b = 60 mm to 93.5 mm at near beam-ends, in order to overcome shear forces developed by the reactions on supports. This variation happens on a length of 335 mm, the length of widened beam portion becoming equal to 1015 mm, about 1/5 of the total bridge length[4]. The depth of main beam is h = 300 mm.

The cross section of widened main beam at support, together with an end floor beam is shown on the left side of Fig.1. The right side of the same figure shows the cross section of main beam at midspan and an intermediate floor beam. Main beams are doubly reinforced by two sets of vertically inserted, glued-in steel ribs. The compression reinforcement is a single rib of 3x44 mm, while the tension reinforcement is made up of two ribs, each having a cross section of 6x70 mm.

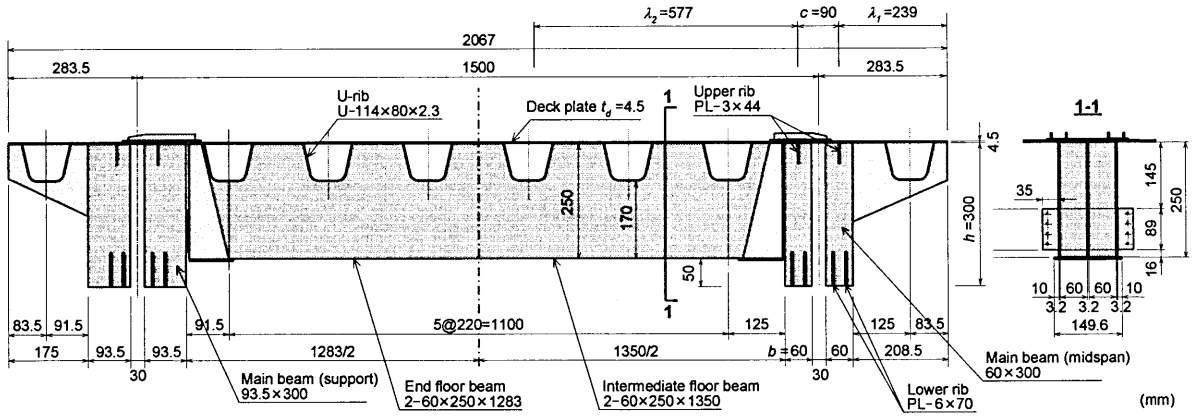

Fig.1 Bridge model cross section (left: support, right: midspan)

The applied wood material was Japanese cedar of strength grade E75-F240 JAS (Japanese Agricultural Standard), while steel was SS400. A measured value of bending moment capacity of Japanese cedar glulam was used for calculations, being equal to $\sigma_{y,W}$ = 39 MPa. The measured modulus of elasticity of Japanese cedar glulam is E_W = 9 GPa, the shear modulus is G_W = 601 MPa. The measured yield strength $\sigma_{y,S}$ = 297 MPa and the allowable bending stress σ_{ba} = 137 MPa was used for SS400. The modulus of elasticity of steel equals E_S = 206 GPa. The bridge was designed using the plastic composite beam theory, where all steel is converted to an equivalent wood area, resulting in a transformed section[4].

Prior to failure test, this model was subjected to nine bending tests, corresponding to nine loading cases. The difference between these cases was the position of the applied truck wheel load[2]. A load-controlled testing machine loaded the simply supported model. Results of one of the bending tests (at load case LC1) and of the failure test (at load case LC2) are presented in Chapter 4. of this paper. A total number of one hundred strain gauges were installed at four different cross sections along the hybrid bridge model. At section B-B (midspan) gauges were installed to the bottom of floor beams, to steel side plates and to lower inserted ribs. At sections C-C (350 mm from midspan) and D-D (Fig.13) gauges were applied along the depth of main beams, to the upper surface of orthotropic steel deck and to the bottom of U-ribs[3].

3. FINITE ELEMENT ANALYSIS

The inserted steel rib on the compression side of the glulam main beams serves as shear connector between the deck plate and the main beams, while the role of the glued-in steel ribs on the tension side of the main beams is to compensate the longitudinal axial strength. Thus, a part of the steel deck (determined by the effective widths λ_1 = 239 mm and λ_2 = 577 mm, obtained by applying the Japanese shear lag formula for roadway bridges), the upper and lower ribs and the double glulam main beam form a composite beam. Therefore the plastic composite beam theory could be used to calculate the bending and shear stresses[4]. The composite beam was defined as the glulam-steel hybrid structure within width $\lambda_1 + c + \lambda_2$ (see Fig.1).

Performing a 3-D finite element analysis represents the next step in understanding the behavior of the proposed timber-steel hybrid structure. In addition to the already existing experimental and analytical study, finite element calculations were performed by ANSYS Academy Teaching Introductory v11.0, which is a general purpose FEM package. Among other mechanical problems, the ANSYS package can be utilized for static non-linear structural analysis. Considering the loading scheme during testing and taking advantage of the geometric symmetry, only half of the tested structure was modeled (see Fig.4 and Fig.8). Symmetry boundary conditions were applied at midspan and the structure was simply supported.

In order to obtain reliable results in FEM, accurate modeling of material properties is important. Japanese cedar glulam was of strength grade E75-F240, steel was SS400 (Fig.2). Glulam was modeled as an elasto-plastic orthotropic material with a bilinear stress-strain curve, using a bending moment capacity equal to $\sigma_{y,W}$ = 39 MPa. The following values of modulus of elasticity, shear modulus and Poisson's ratio were used: E_Z = 9 GPa, E_X = E_Y = 300 MPa, G_{YZ} = G_{XZ} = 601 MPa, G_{XY} = 60 MPa, ν_{YZ} = ν_{XZ} = 0.01, ν_{XY} = 0.2, where Z-axis is parallel to grain. Steel was modeled as a perfect elasto-plastic isotropic material, with the values E_S = 206 GPa, ν_S = 0.3, together with a yield strength of $\sigma_{y,S}$ = 297 MPa. The applied truck wheel load was modeled as a pair of uniformly distributed loads. The geometric model was used to create a mesh of 8-node solid elements with different sizes, comprising 21,266 elements and 21,170 nodes in total[5), 6)].

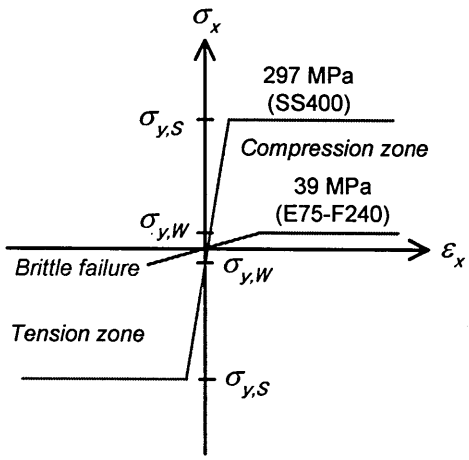

Fig.2 Applied material models

4. RESULTS AND DISCUSSIONS

4.1 Load case LC1

Prior to failure test in load case LC2, the model shown in Fig.3 was subjected to bending in load case LC1. A half-structure three-dimensional model (Fig.4) was created for this load case. Fig.5 shows the deformed shape of the FEM model at midspan (magnified 10 times for better visibility) at load P = 120 kN.

Measured and calculated deflections are shown in Table 1 and compared in Fig.6. In the test, glulam floor beams and main beams were not connected to each other in order to check the effectiveness of the special structural members (situated on top of the main beams) used for load transfer from floor beams to main beams, as shown in Fig.1. At this stage of the FEM analysis, these members were not modeled yet. In the test, as well as in the analysis, double glulam floor beams are connected to the steel deck plate only. There is a disagreement between the two sets of values, because the special structural members responsible for load transfer from floor to main beams (Fig.1) were not modeled at this stage.

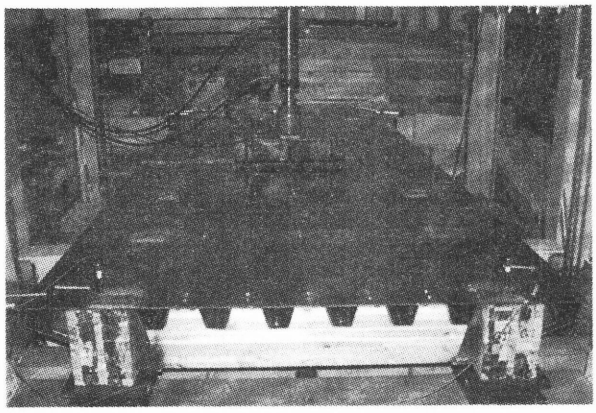

Fig.3 Bridge model in LC1

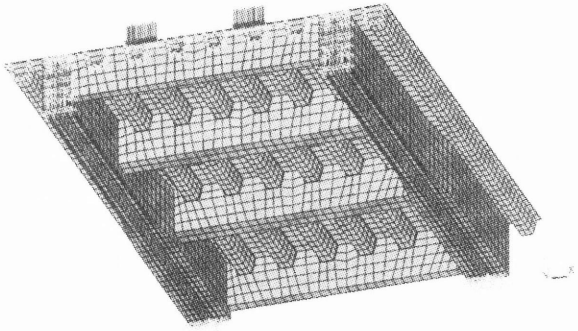

Fig.4 Finite element model in LC1

Table 1 Deflections for load case LC1

Cross section	Deflection meter	δ(mm)	
		Test	FEM
B−B	CH2	8.4	7.5
	CH1	8.3	7.5
C−C	CH5	13.8	15.1
	CH4	13.5	15.0
	CH3	13.9	15.1

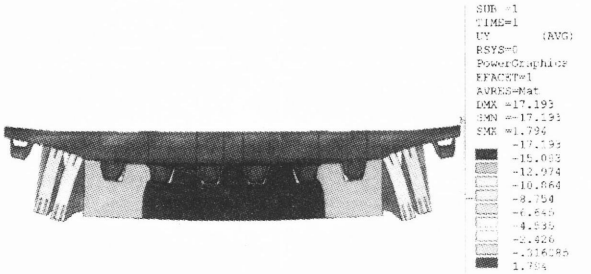

On the right: vertical deflection (UY) values in mm

Fig.5 Deformed shape at P = 120 kN (magnified 10 times)

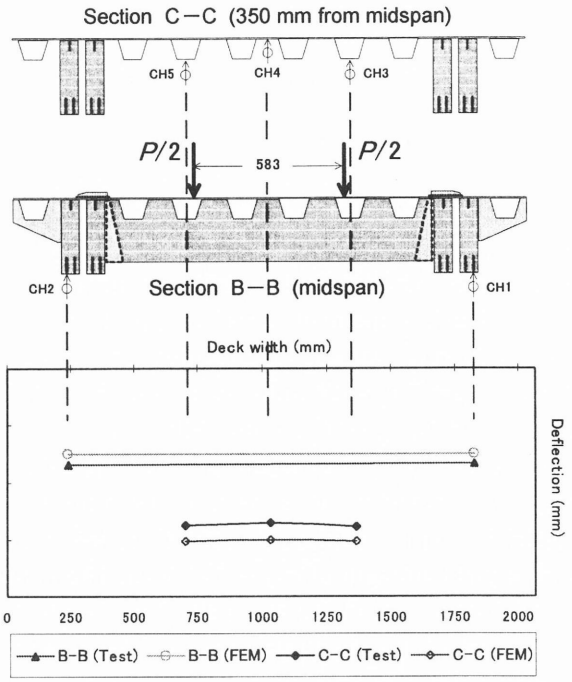

Fig.6 Deflection distribution at P = 120 kN

4.2 Load case LC2

After bending tests performed in load case LC1 and the other load cases[2], the failure test in load case LC2 took place (Fig.7). The corresponding FEM model is shown in Fig.8. Based on the applied material models, a non-linear static analysis was performed. Fig.9 shows the bridge model during testing at yield load P_Y and ultimate load P_U, while Fig.10 shows the accompanying load-deflection curves, capturing only a portion of the ductile experimental curve[3].

Calculated P-δ curves determined for deflection meters CH2 and CH1 at midspan by the plastic composite beam theory (PCBT), along with curves resulted from the FEM analysis are included here, the latter being in good agreement with the measured ones. Yield load P_Y, plastic load P_P and ultimate load P_U was determined by the plastic composite beam theory[4]. Plastic composite beam theory assumes that at yield load P_Y, the steel of lower rib at deflection meter CH2 reaches its yield strength and starts to yield: in the FEM analysis, this happened at a load larger than the assumed yield load.

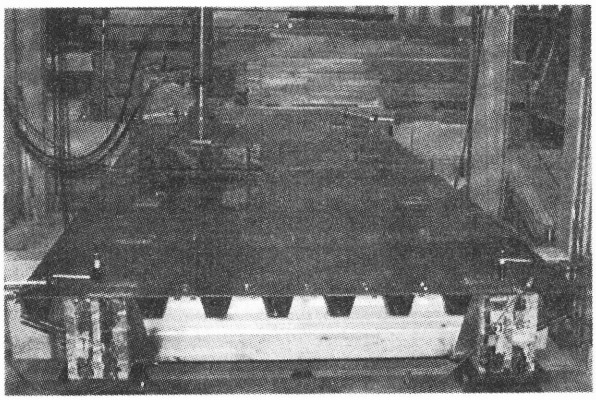

Fig.7 Bridge model in LC2

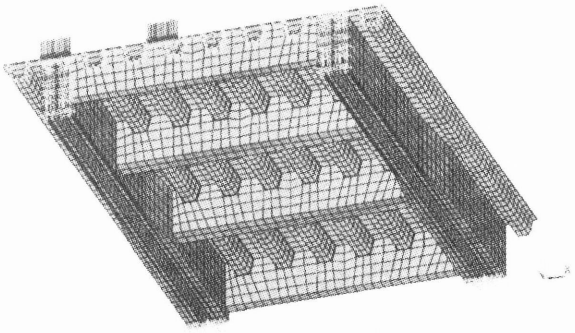

Fig.8 Finite element model in LC2

However at plastic load P_P, the whole lower rib at midspan was in fully plastic state, as assumed by the PCBT. At ultimate load P_U, the glulam of main beam at deflection meter CH2 did not reach its modulus of rupture as predicted by the PCBT: in the FEM analysis, this happened at the experimental ultimate load $P_{U,exp}$, being the load where ductile failure of the structure started to begin during testing.

Failure of the bridge model occurred in a ductile manner, based on the observed failure mechanism. Eight distinct failure positions were detected during the test[4]. Flexural failure started from a knot situated at the tension side of main beam G4, near midspan (Fig.13). Then failure propagated due to a horizontal crack, close to the first failure position. Glue line represented a major a cause of premature failure, because the next failure is due to the separation of glulam and glue from the lower ribs of main beam G3. The fourth, fifth and sixth positions also exhibited flexural failure. Shear failure occurred at the seventh position, close to the neutral axis, just as at the eighth (final) failure position. Up to the seventh position, deck plate and U-ribs were in elastic state. But at the final position, U-ribs were already in plastic state.

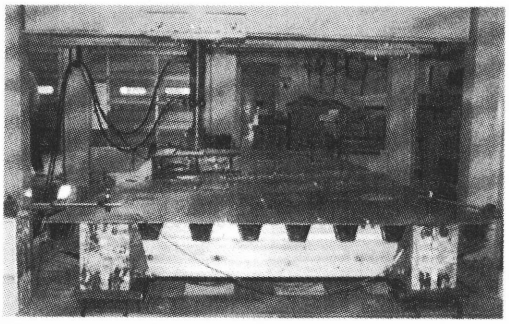

At load P_P=179 kN

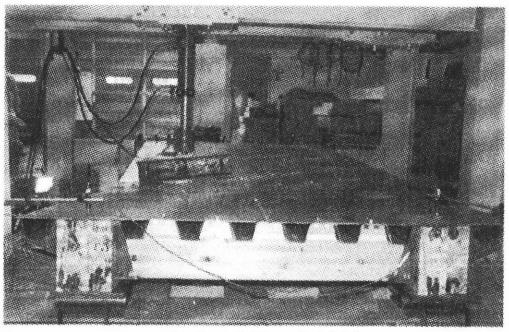

At load P_U=244 kN

Fig.9 Bridge model during loading

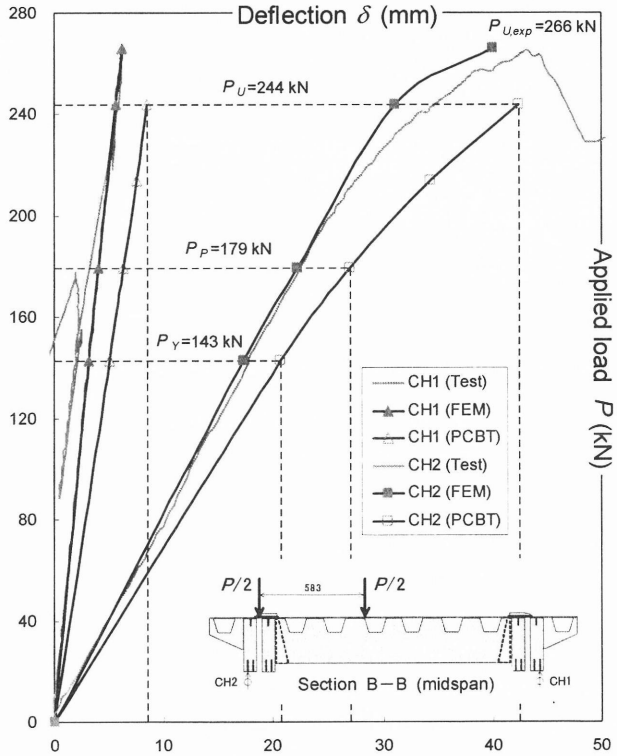

Fig.10 Load-deflection curves (detail)

Deformed shape of hybrid structure at midspan (shown in Fig.11) is obtained from the FEM analysis under each applied truck wheel load P_N ($N = Y, P, U$), calculated by the plastic composite beam theory. Note that deformed shapes from the FEM analysis are magnified 10 times to provide better visibility. Fig.12 shows deflection distributions at loads P_N ($N = Y, P, U$). Three sets of deflection are included: first, experimental deflections of main beams G4 and G2, measured at section B-B by deflection meters CH2 and CH1, as well as experimental deflections of U-ribs, measured at section C-C by deflection meters CH3, CH4 and CH5 are shown. Then, deflection values calculated by FEM analysis are included for the same sections. Finally, for glulam main beams at section B-B, deflection values determined analytically by the plastic composite beam theory (PCBT) are also included.

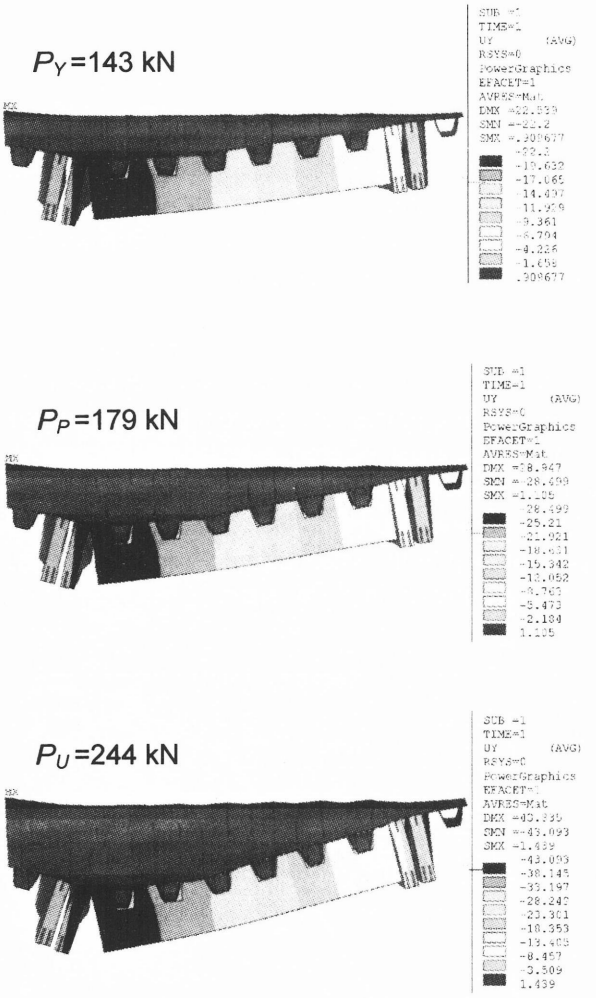

Fig.11 Deformed shape at applied loads (magnified 10 times)

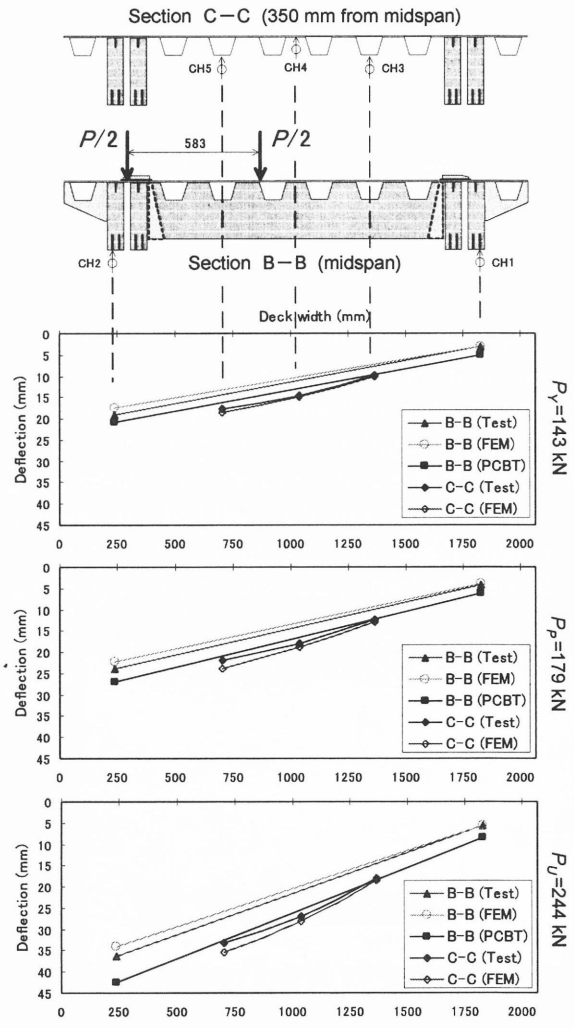

Fig.12 Deflection distribution at P_N ($N = Y, P, U$)

Comparing these three sets of values to each other, a good agreement can be observed, calculated values from the FEM analysis closely following the measured data. Compared to measured deflections, deflections obtained from FEM are larger for U-ribs and smaller for main beams due to a simplified approach in the analysis, regarding connection between structural members. All deflection values used to construct Fig.12 are shown in a tabulated form in Table 2. In addition to the deflection data at applied truck wheel load P_N ($N = Y, P, U$), measured deflections and deflections calculated by the FEM analysis are also included for the experimental ultimate load $P_{U,exp}$, to demonstrate the good agreement between the two sets of data. For section C-C, deflections calculated by the plastic composite beam theory are not available.

Table 2 Measured and calculated deflection values at applied loads for load case LC2

Cross section	Defl. meter	P_Y = 143 kN			P_P = 179 kN			P_U = 244 kN			$P_{U,exp}$ = 266 kN	
		δ(mm)			δ(mm)			δ(mm)			δ(mm)	
		Test	FEM	PCBT	Test	FEM	PCBT	Test	FEM	PCBT	Test	FEM
B−B	CH2	19.3	17.3	20.7	23.9	22.2	27.0	36.3	31.1	42.4	44.6	40.0
	CH1	3.2	3.1	5.0	4.1	4.0	6.3	5.7	5.6	8.5	6.2	6.1
C−C	CH5	17.8	18.6	N/A	21.9	23.8	N/A	33.1	35.5	N/A	40.0	40.9
	CH4	14.6	14.8	N/A	18.1	18.9	N/A	26.9	28.0	N/A	32.1	32.0
	CH3	9.9	10.0	N/A	12.3	12.8	N/A	17.9	18.5	N/A	20.9	21.0

Fig.13 presents a lateral view of longitudinal strain distribution of glulam main beams at the ultimate load P_U = 244 kN, determined by the plastic composite beam theory. Measured and calculated strain values are included, FEM strain distribution following closely the measured one. For G4 and G3, measured strain values and strains determined by the FEM analysis are also included for the deck plate and lower rib at each section considered. Composite action could not be achieved completely between deck plate, glulam beam and lower ribs, therefore differences between strain values of these members occurred.

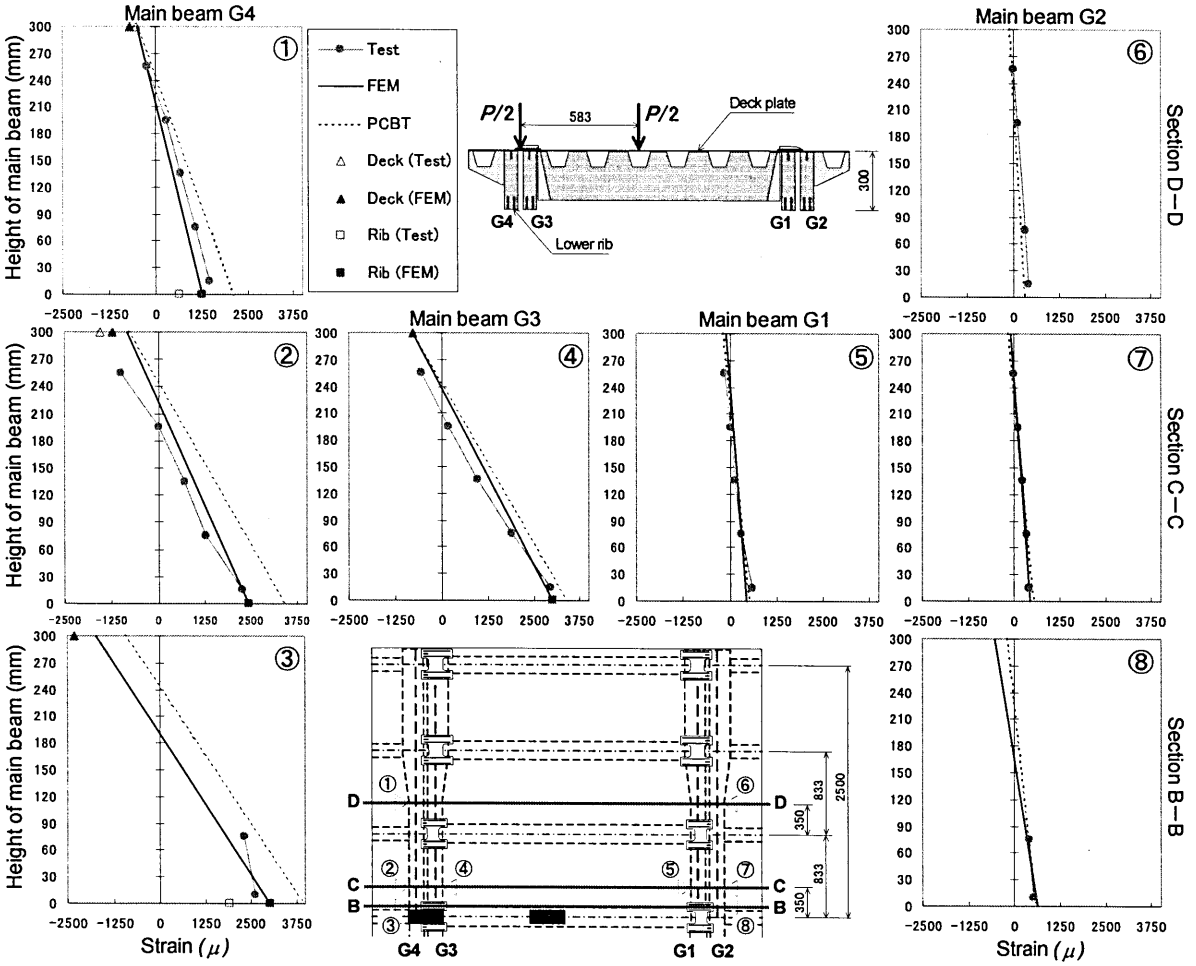

Fig.13 Longitudinal strain distribution of glulam main beams at P_U = 244 kN (lateral view)

5. CONCLUSIONS

Test results of a one-third-scale hybrid bridge model showed that the plastic composite beam theory could not predict closely enough the behavior of the tested bridge model. Therefore, in addition to this approach, a non-linear three-dimensional FEM analysis was performed to describe more accurately the performance of the structure. Since several details from the tested structure are not yet included in the FEM model, further work is needed to obtain a more thorough view of the behavior of the hybrid bridge structure considered. In the failure test, glue line represented a major cause of premature failure: while glue was not modeled this time, it also needs to be modeled in the future, since glue stiffness, thickness, etc. seems critical for this hybrid structure.

The authors intend to model the entire tested structure as shown in Fig.14, so they will be able to perform analyses for the remaining load cases, too[3]. Due to the limited node and element number capabilities of the ANSYS University Intermediate package, this model can only be achieved by converting the double glulam floor beams to equivalent single steel floor beams, modeling them as 4-node elastic shell elements. The steel deck plate, U-ribs and inserted steel ribs will also be modeled by shell elements. Double glulam main beams will be modeled by 8-node solid elements, but applying a finer mesh compared to the one used in this paper. Also the effectiveness of the special structural members (situated on top of the main beams) used for load transfer from floor beams to main beams will be checked. The authors wish to present the results of these new analyses in a future paper.

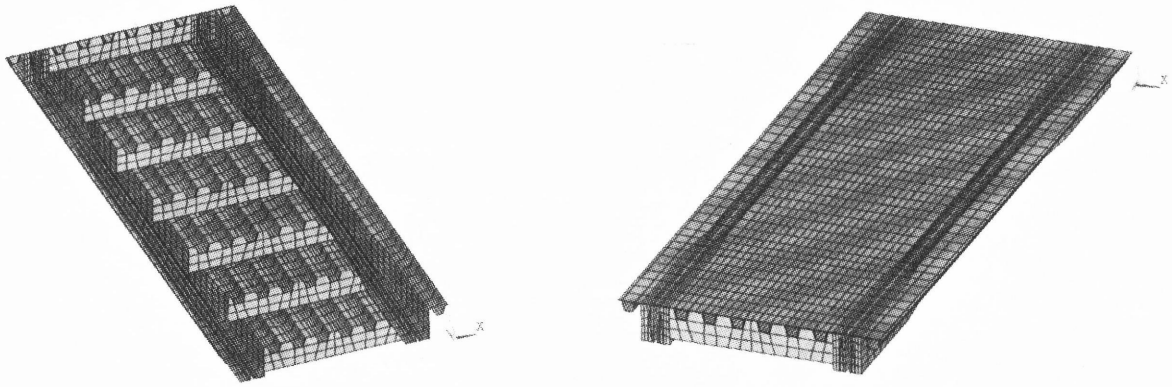

Fig.14 Finite element model of full-structure

6. REFERENCES

1) Kiss, L., Sasaki, T., Usuki, S., Finite element modeling of timber-steel hybrid bridge, *Proceedings of the 62nd Annual Conference of the Japan Society of Civil Engineers*, 2007 (to be published)
2) Kiss, L., Sasaki, T., Toyota, A. and Usuki, S., Performance of glulam beam-orthotropic steel deck hybrid bridge structure, *Proceedings of the 9th World Conference on Timber Engineering*, 2006
3) Kiss, L., Sasaki, T., Usuki, S., Behavior of glulam beam-orthotropic steel deck hybrid bridge structure, *Proceedings of the 5th Symposium on Timber Bridges, JSCE*, pp. 101-106, 2006
4) Kiss, L., Usuki, S. and Sasaki, T., Experimental and analytical study on steel deck-glulam beam hybrid bridge behavior, *Journal of Structural Engineering, JSCE*, Vol. 51A, pp. 1211-1218, 2005
5) Miki, C., Suganuma, H., Tomizawa, M., Machida, F., Cause study on fatigue damage in orthotropic steel bridge deck, *Proceedings of the Japan Society of Civil Engineers*, No. 780, I-70, pp. 57-69, 2005 (in Japanese)
6) Pousette, A., Full-scale test and finite element analysis of a wooden spiral staircase, *Holz als Roh- und Werkstoff (European Journal of Wood and Wood Products), Springer-Verlag*, Volume 61, pp. 1-7, 2003